Mesoporous carbons with KOH activated framework and their hydrogen adsorption

Minkee Choi and Ryong Ryoo*

Received 19th March 2007, Accepted 29th June 2007
First published as an Advance Article on the web 10th August 2007
DOI: 10.1039/b704104g

The effects of KOH activation on pore structure of ordered mesoporous carbons were analyzed by transmission electron microscopy, powder X-ray diffraction and argon adsorption. The activation led to remarkable increases in micropore volume and BET surface area up to 1.0 mL g^{-1} and 2700 m^2 g^{-1}, at the expense of the mesostructural order. The resultant carbons with various microporosity and mesoporosity were tested for room-temperature adsorption of hydrogen under high pressure. The adsorption data were analyzed in correlation with the varied carbon pore structures. The results showed that the hydrogen adsorption capacity increased approximately linearly with respect to micropore volume, or BET surface area, reaching a 2.5-times higher value when fully activated. However, the adsorption capacity at 100 atm (0.75 wt%) was still far below the US DOE target of 6.5 wt%. The extrapolation of our results to the carbon structure with the highest possible surface area could lead to no more than 2.5 wt%. This result suggests that chemisorption or other chemical storage methods should be combined with physisorption if carbon materials are considered for hydrogen storage.

1. Introduction

Nanostructured carbons have attracted much scientific attention in recent years, due to their possibilities as adsorbents, catalyst supports, composite materials and sensor electrodes. In particular, ordered mesoporous carbons, synthesized using mesoporous silica templates,[1–5] were considered as catalyst supports,[3] adsorbents for bulk molecules,[6,7] supercapacitor electrodes,[8,9] hydrogen storage materials[10] and synthesis templates for other nanostructured materials.[11,12] Such mesoporous carbons are attractive due to their large surface area, facile molecular transport and high dispersion of supported metal. Mesoporosity of the carbons (*i.e.*, pore diameters and connectivity) was controlled *via* the use of silica templates that were designed into various structures and framework thicknesses.[1–5,10] Some of the mesoporous carbons were imparted with a certain level of microporosity[10] that was coincidentally generated inside the mesoporous frameworks during the carbon synthesis. Microporosity is important in various applications of carbons such as the preparation of supported metal nanoparticles, gas adsorption and electrical energy storage in the carbon materials. However, no systematic ways to control microporosity of the mesoporous carbons have previously been developed. Here, we investigated the effects of chemical activation using KOH as a means of generating framework microporosity in mesoporous carbons. We chose a mesoporous carbon with cubic *Ia3d* structure (previously referred to as CMK-8)[4] as a starting material as its 3-dimensional pore connectivity was suitable for facile diffusion of the activating agent. We also evaluated the resultant carbons with controlled mesoporous/microporous textures for the reversible storage of hydrogen using physisorption at room temperature.

The chemical activation with KOH and NaOH is a well-established method that can be used to generate highly microporous carbon structures from various carbonaceous materials such as coal,[13] bitumen,[14] anthracite,[15] and nanotubes.[16] The carbonaceous materials are heated with the alkali hydroxide to a high temperature, where the alkali species is reduced to metal by the carbon framework.[17] The carbon framework is etched to generate pores, due to the oxidation of carbon into carbonate ion. These processes lead to the generation of micropores, and subsequently, the alkali metal species is removed by acid washing. The activation process provides several advantages over conventional activation processes using steam or CO_2 at high temperature.[18] For instance, the alkali activation allows higher yield, lower processing temperature, shorter treatment time, and more uniform and higher microporosity. The alkali activation process is suitable for the preparation of very highly microporous carbons possessing extremely high BET surface areas (up to 3000 m^2 g^{-1}), which are called 'superactivated carbons'. Such microporous carbons with extremely high micropore volumes and BET surface areas have recently attracted attention for hydrogen storage.

In recent years, hydrogen was considered as a clean energy medium that could revolutionize our economy from the dependence on fossil fuels. Hydrogen is, however, not a convenient energy medium as its storage and transportation are difficult and costly. Currently, the main bottleneck of the 'hydrogen economy' is the difficulties in the storage of hydrogen at a sufficiently high energy density that can meet the DOE goal for automotive fuel cell systems (*i.e.*, 6.5 wt%). Various storage technologies have been proposed to achieve a safe and economic way to store hydrogen, which include high pressure compression, physisorption on nanoporous

Centre for Functional Nanomaterials, Department of Chemistry, Korea Advanced Institute of Science and Technology, Daejeon, 305-701, Republic of Korea. E-mail: rryoo@kaist.ac.kr; Fax: +82-42-869-8130; Tel: +82-42-869-2830

 This journal is © The Royal Society of Chemistry 2007

adsorbents, and formation of metal hydrides.[19] Among the methods, room-temperature adsorption on nanoporous carbons was extensively studied due to the economic feasibility, fast kinetics and complete reversibility of the storage process. Many recent studies on hydrogen adsorption using carbon adsorbents were motivated by earlier measurements reporting very striking capacities, such as 60 wt% on graphitic nanofibers,[20] and 5–10 wt% on carbon nanotubes.[21] However, the high adsorption capacities have never been reproduced, nor explained by theoretical calculations.[22–24] In 1999 Chen *et al.* reported a large hydrogen uptake (up to 20 wt%) for alkaline metal treated carbons.[25] However, their results have been reinvestigated by Yang *et al.*[26] and most of the weight uptake was attributed to the moisture from the hydrogen gas stream. At present, the independently confirmed and reproducible storage capacities with carbon materials appears to be less than 1 wt%. Nevertheless, many people still seem to believe that nanoporous carbons would be good for hydrogen storage.

In the present work, we investigated the hydrogen adsorption capacity of the aforementioned KOH-activated mesoporous carbons. We built a high-accuracy gravimetric apparatus based on a magnetic suspension microbalance for reliable measurements of the hydrogen capacity (with a maximum error range of 0.03 wt%).[27] Compared with volumetric methods, the gravimetric method can provide direct gas uptake measurement without the problems of high-pressure hydrogen leakage and temperature variations caused by adiabatic gas expansion.[27] The measurement data were analyzed in correlation with carbon structural properties such as BET area and micropore volume, in order to clarify if carbon adsorbents are really suitable for reversible hydrogen storage at room temperature. In particular, by extrapolating such correlations to the maximum possible carbon surface area, we tried to evaluate the feasibility of hydrogen storage based on carbon adsorbents. The results are provided to increase our insights for the design of suitable hydrogen storage systems.

2. Experimental

2.1. Material preparation

A mesoporous silica sample with cubic *Ia3d* structure (designated as KIT-6) was prepared according to the hydrothermal synthesis procedure using tetraethoxysilane and polyalkyleneoxide-type block copolymers.[4] The KIT-6 silica was used as a template for syntheses of two kinds of mesoporous carbons with the same cubic *Ia3d* mesostructure but different framework microstructures. The carbon with a graphitic framework (referred to as CMK-8G) was synthesized using acenaphthene as a carbon precursor.[5] The other carbon with an amorphous framework (referred to as CMK-8) was synthesized using sucrose as a carbon source.[4]

The KOH activation was performed by heating a carbon–KOH physical mixture under N_2 flow (120 mL min^{-1}). As a starting carbon material, mesoporous carbon with an amorphous framework (synthesized using sucrose) was used. The activation temperature was increased to 1023 K with a 5 K min^{-1} gradient and maintained there for 1 h. The KOH/carbon mass ratio was varied in the range between 0 and 5, for control of the degree of activation. After heating with KOH, the mixture was washed three times with 3 M hydrochloric acid at room temperature and once with distilled water. The resultant samples were dried at 373 K. Hereafter, the carbon samples are denoted as A*n*-CMK-8, in which A means 'activated', and *n* indicates the KOH/carbon mass ratio.

2.2. Characterization

Powder XRD patterns were recorded with a diffractometer operating with Cu Kα radiation at 1.6 kW (Rigaku Multiplex). For transmission electron microscopy (TEM), the powder samples were dispersed in ethanol with sonication. Porous carbon grids were dipped into the suspension, and the dried grids were used for the investigation. TEM images were obtained with a Philips F20 Tecnai instrument operating at 160 kV. The argon adsorption isotherms were measured at 87.3 K using an ASAP2020 (Micromeritics) gas adsorption analyzer. The micropore volume and the size distribution were calculated by applying the Dubinin–Radushkevich equation[28] and the Horvath–Kawazoe method,[29] respectively. The mesopore size distribution was analyzed with a desorption branch using the BJH algorithm.[30]

2.3. Measurement of the hydrogen gas adsorption capacities

Hydrogen adsorption capacities for various nanoporous materials were measured under high-pressure conditions (up to 100 atm) at 298 K. By considering that a reliable measurement of the adsorption capacity is essential for achieving accurate evaluation of the material, a detailed description of the measurement procedure is given. For the measurements, a gravimetric analysis system (Fig. 1) equipped with a magnetic suspension microbalance (Rubotherm) with 10^{-5} g sensitivity was built in a laboratory.[27] Blank runs were performed with an empty cell in order to calibrate the buoyancy of the

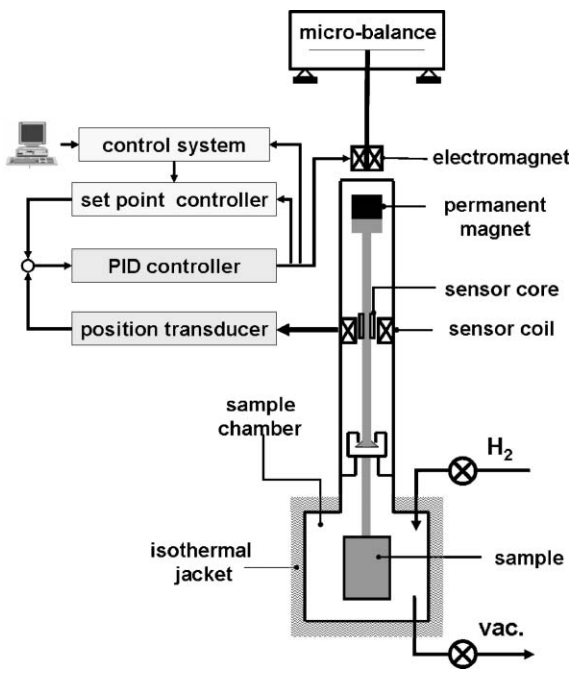

Fig. 1 Schematic diagram of the gravimetric hydrogen adsorption apparatus.

high-pressure gases on the empty cell and cell holder. For the determination of buoyancy on the samples, the sample framework densities were predetermined by He pycnometry and the Redlich–Kwong gas equation was used for the determination of gas densities. For the measurement, approximately 0.1 g sample was used after degassing at 573 K for 12 h. During the measurement of the adsorption isotherm, the temperature of the measurement system was maintained at 298 K *via* water circulation. Hydrogen was introduced to the desired pressure, and when thermodynamic equilibrium was reached, the amount of adsorbed gas was calculated by measuring the weight changes of the samples. At each point, the sample weight was measured three times and averaged.

3. Results and discussion

3.1. KOH activation of the ordered mesoporous carbon

TEM investigation (Fig. 2) and well-defined low angle XRD patterns (Fig. 3) reveal that pristine mesoporous carbon contains the highly ordered cubic *Ia3d* mesoporous structure.[4] As shown in the XRD patterns, KOH activation leads to a gradual decrease in low-angle XRD peak intensity as the degree of activation (*i.e.* KOH/carbon mass ratio) increases. This result indicates that the KOH activation induces significant structural transformation of the carbon framework, causing a loss of long-range mesostructural order. High-resolution TEM investigation (Fig. 2) also confirms that ordered pore arrangement of pristine mesoporous carbon (CMK-8) gradually disappears with KOH activation. At a KOH/carbon ratio of 1 (A1-CMK-8), most of the ordered mesoporous domain is still retained, while the carbon framework locally contains a large amount of disordered microporous structure. As the KOH/carbon ratio increases above 3, most of the ordered mesoporous domain is transformed into a highly microporous structure.

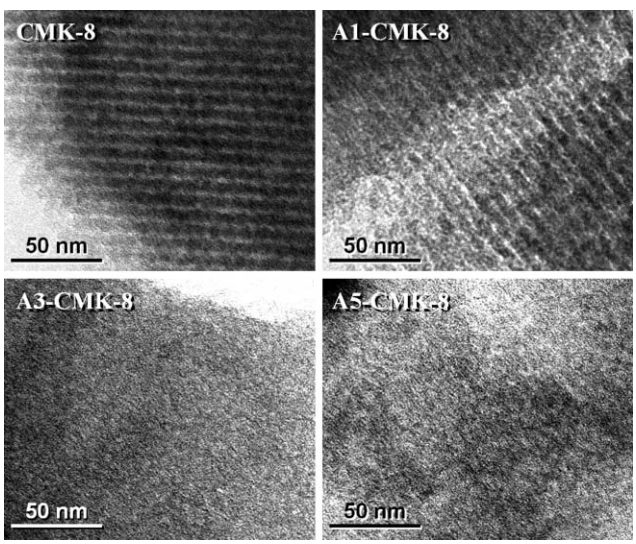

Fig. 2 TEM images of pristine and KOH activated mesoporous carbons. CMK-8 is pristine mesoporous carbon having an ordered pore arrangement with cubic *Ia3d* symmetry. KOH activated carbons are denoted as A*n*-CMK-8, in which A means 'activated', and *n* indicates the KOH/carbon mass ratio.

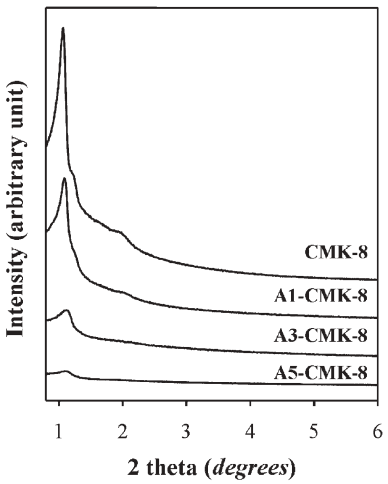

Fig. 3 Low-angle powder X-ray diffraction patterns of pristine and KOH activated mesoporous carbons.

In Fig. 4, the argon adsorption isotherms and pore topological properties of pristine and activated carbons are shown. The argon adsorption isotherm of pristine mesoporous carbon is essentially type IV according to the IUPAC classification. The pristine mesoporous carbon exhibits a large mesopore volume (0.79 mL g^{-1}) with a narrow pore size distribution (4.2 nm) due to the ordered mesoporous structure. The pristine mesoporous carbon also contains considerable amounts of micropores (0.31 mL g^{-1}), although the micropore size distribution is rather broad. Such microporosity can be

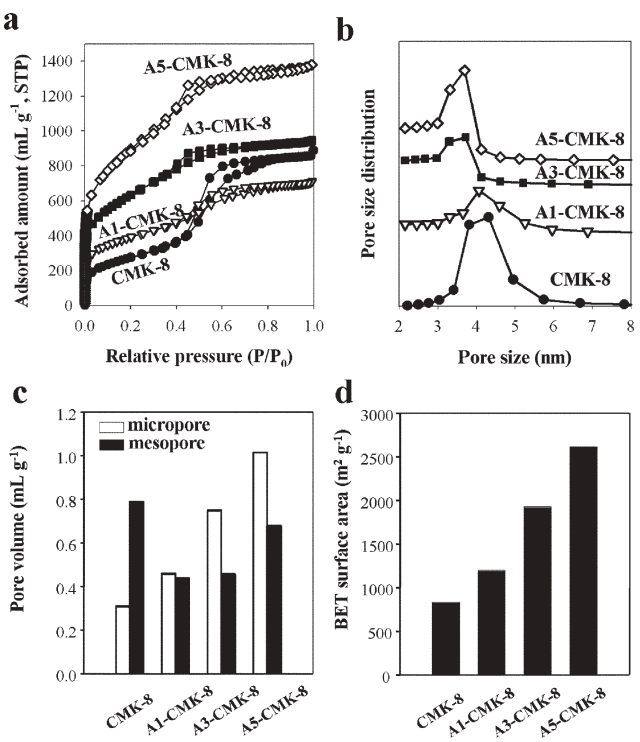

Fig. 4 Argon adsorption isotherms and pore textural properties of pristine and KOH activated mesoporous carbons: a) argon adsorption isotherms, b) mesopore size distribution, c) micropore and mesopore volume, and d) BET surface area.

This journal is © The Royal Society of Chemistry 2007

Table 1 Pore textural properties of various carbon materials that were evaluated for hydrogen storage

Sample	S_{BET}[a]/m^2 g^{-1}	V_{micro}[b]/mL g^{-1}	V_{meso}[c]/mL g^{-1}	V_{total}[d]/mL g^{-1}	w_{BJH}[c]/nm	d_{HK}[e]/nm
CMK-8G	261	0.11	0.30	0.41	3.4	0.87
CMK-8	833	0.31	0.79	1.10	4.2	0.87
A1-CMK-8	1200	0.46	0.44	0.90	4.1	0.79
A3-CMK-8	1930	0.75	0.46	1.21	3.7	0.82
A5-CMK-8	2700	1.00	0.68	1.70	3.7	0.84

[a] S_{BET} is the BET surface area. [b] V_{micro} is the micro pore volume determined by using the Dubinin–Radushkevich equation.[28] [c] V_{meso} is the mesopore volume equal to $V_{total} - V_{micro}$; w_{BJH} is the mesopore diameter calculated using the BJH method.[30] [d] V_{total} is the pore volume at a relative pressure of 0.95. [e] d_{HK} is the median micropore diameter calculated by the Horvath–Kawazoe method.[29]

ascribed to the use of sucrose as carbon precursor for the mesoporous carbon synthesis. Carbonization of oxygen-rich organic molecules such as sucrose generates a large amount of gaseous species (*e.g.*, CO_2 and H_2O), resulting in the generation of considerable void spaces (*i.e.*, micropores) inside the carbon framework. In contrast, polyaromatic precursors such as acenaphthene and mesophase pitch can produce more graphitic carbon frameworks possessing negligible microporosity.[10]

As shown in Fig. 4, the micropore volume and BET surface area of the carbon dramatically increase after KOH activation. A remarkably high micropore volume (1.0 mL g^{-1}) and BET area (2700 m^2 g^{-1}) can be achieved at a KOH/carbon ratio of 5. Such a large BET surface area has been similarly reported for superactivated carbons.[13,31] It is noteworthy that such a value is as high as the theoretical surface area of a double-sided separated graphitic sheet (2965 m^2 g^{-1}).[32] Compared to the intrinsic micropores of pristine carbon, the micropores generated by KOH activation exhibit much narrower pore size distribution centered at 0.7–0.9 nm (Table 1). Such a micropore size distribution is expected to be advantageous for hydrogen storage, as it includes a large proportion of pores having optimum sizes for hydrogen storage (0.66 nm).[31]

The mesopore volume of the carbon is lowest at a KOH/carbon ratio of 1, but thereafter increases with the KOH loading. The decrease in mesopore volume at low KOH/carbon ratio can be ascribed to the local destruction of the original ordered mesoporous structure. The increasing mesoporosity at high KOH/carbon ratio is attributed to the generation of new type of mesoporous structure. As indicated by the lack of distinct peaks in the XRD patterns (Fig. 3), the newly developed mesoporous structure is completely disordered. Such disordered mesoporous structures seem to be generated by the systematic enlargement or coalescence of the disordered microporous structure. Such a disordered mesopore structure exhibits quite a narrow pore size distribution centered at 3.7 nm (Fig. 4B), which is somewhat smaller than the diameter of the initial ordered mesopores (4.2 nm). A narrow adsorption–desorption hysteresis loop indicates that the disordered mesopores are not isolated or entrapped within the microporous carbon structure, but they are exposed to the external surface of the carbon particle through a 3-dimensional interconnection. The concomitant generation of uniform micro- and mesoporous structure is a unique feature of the KOH activation using ordered mesoporous carbon precursors. It has been reported that activation of bulk carbon precursors such as coal,[13] bitumen,[14] and anthracite[15] leads to carbon materials with mostly microporous structures. Activation of nanostructured carbon materials such as MWNT[16] also produced similar micro-/mesoporous structures, although the pore volume and BET surface area were much smaller.

It is noteworthy that the activation takes place quite uniformly within carbon textures. Careful TEM investigation confirmed that both internal and external domains of carbon particles were homogeneously activated, exhibiting uniform distributions of micropores and mesopores. This indicates that the activating agent KOH is homogeneously distributed within the carbon structure during the activation process. Since the activation temperature (1023 K) is much higher than the melting point of KOH (679 K), KOH would be present as a liquid during the activation process. We believe that the unique ordered mesoporous structure of carbon precursor allows facile diffusion of the liquefied KOH *via* capillary interaction, which induces such homogeneous structural transformation of carbon textures.

3.2. Hydrogen storage on activated mesoporous carbons

The pore textural properties of carbon materials studied for hydrogen adsorption are summarized in Table 1. All the hydrogen adsorption isotherms measured at 298 K exhibit typical Langmuir-type (type I according to IUPAC classification) shapes (Fig. 5). Fast kinetics and complete reversibility of the adsorption process indicate that the interaction between hydrogen and the carbon surface is due to a physical

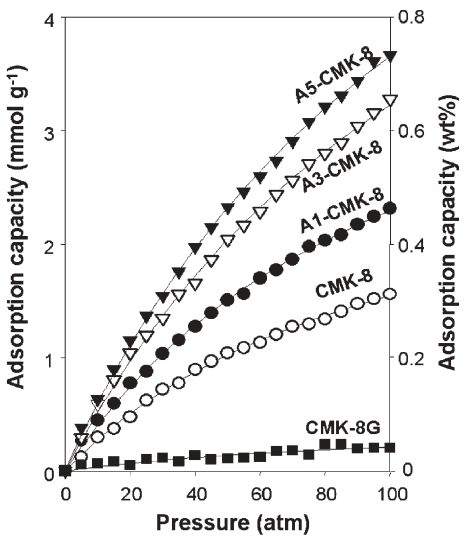

Fig. 5 Hydrogen adsorption isotherms of various carbon materials, measured at 298 K using a gravimetric analysis apparatus.

adsorption process. The hydrogen adsorption capacity markedly increases with the activation of the mesoporous carbon. As clearly shown in Fig. 6, the carbon materials exhibit hydrogen capacities that are linearly proportional to the BET surface area and micropore volume. Similar correlations have been observed with other nanostructured carbon materials.[13,31,33] Such linear correlations demonstrate that carbon materials ideal for hydrogen storage should possess high microporosity and BET surface area.

To investigate the adsorption capacities of a solely mesoporous carbon structure without microporosity, graphitic mesoporous carbon (denoted as CMK-8G) was also synthesized by using acenaphthene as a carbon precursor.[5] It is noteworthy that CMK-8G, which has high mesoporosity but negligible microporosity, exhibits a very small hydrogen adsorption capacity. This result is consistent with the theoretical calculation indicating that only micropores with small pore diameters can make a significant contribution to hydrogen adsorption.[22]

Among the materials studied in the present work, the mesoporous carbon with the highest activation degree (A5-CMK-8) shows the largest hydrogen capacity: 0.75 wt% at 100 atm. This is 2.5 times higher than the value of 0.3 wt% of pristine mesoporous carbon. Unfortunately, the adsorption capacity is still insufficient to meet the DOE target of 6.5 wt%. In our experiments, the slope of the linear correlation between the BET area and hydrogen capacity (Fig. 6a) is 1.6×10^{-3} mmol m^{-2} (3.2×10^{-4} wt% m^{-2} g) at 100 atm. This corresponds to a surface coverage of only 14%, assuming the density of liquid hydrogen.[33] The result indicates that the weak van der Waals interaction between hydrogen and the carbon surface is not strong enough to overcome the thermal motion of hydrogen molecules at room temperature.[23] Recently, several research groups have also independently confirmed that hydrogen storage on nanoporous carbons is less than 1 wt% at 100 atm,[31,33] although the BET surface area is as high as the theoretical surface area of a double-sided graphitic sheet (2965 m^2 g^{-1}).[32]

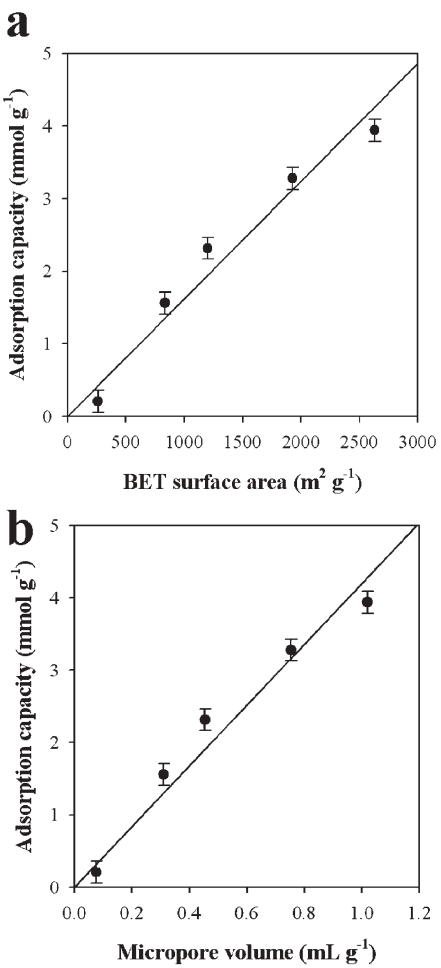

Fig. 6 Hydrogen adsorption capacities *versus* (a) BET surface area and (b) micropore volume of carbon materials. The adsorption capacities were determined at 100 atm.

Accordingly, the question arises: what is the maximum hydrogen capacity achievable with a carbon adsorbent? This question is important to answer, as it may provide valuable insights into the development of feasible hydrogen storage systems. If the density of physisorbed hydrogen is assumed as constant over various carbon pore structures, the maximum possible hydrogen capacity can be roughly expected by the extrapolation of the linear correlation in Fig. 6a. This assumption seems reasonable, as the hydrogen adsorption is depending on the extremely short-range van der Waals interaction between hydrogen molecules and the carbon surface. Panella *et al.*[33] confirmed that activated carbons and single-walled carbon nanotubes exhibited a single linear correlation between hydrogen capacity and BET area, despite their very different pore geometry and surface nature. Such results support that the extrapolation of the linear correlation can be used to generally predict the adsorption capacities of carbon adsorbents. Theoretical work by Chae *et al.* showed that the surface area of carbonaceous materials can be increased to 7745 m^2 g^{-1} when the graphene sheet is fully decomposed into separate benzene rings.[32] Although it is very difficult to achieve, the surface area of separated benzene molecules is the maximum surface area that can be imagined with carbon-based materials. If the linear correlation in Fig. 6a is extrapolated to this surface area, 2.5 wt% (12.5 mmol g^{-1}) hydrogen capacity is obtained at 100 atm. Unfortunately, this value is still much smaller than the DOE target of 6.5 wt%. The result clearly shows that hydrogen storage using room temperature physisorption on carbon adsorbents would be inappropriate to meet the current target for hydrogen storage. Recently, a theoretical calculation using a Grand Canonical Monte Carlo simulation also showed that hydrogen storage on graphitic slit-like carbon pores clearly does not meet the DOE target.[34]

From these results, it seems evident that room-temperature physisorption on carbon adsorbents is not feasible as an efficient hydrogen storage route. To achieve sufficiently high capacity by physisorption, cryogenic temperature should be used in order to depress the thermal motion of the hydrogen molecules.[19,33] Alternatively, as demonstrated by Li and Yang,[35] synergistic combination of physical adsorption with chemical processes such as spillover might be promising for enhancing the storage capacity on carbon materials. Electrochemical hydrogen storage on carbon materials[36–38] also could provide a more efficient route to hydrogen storage.

This journal is © The Royal Society of Chemistry 2007

4. Conclusions

Mesoporous carbons with enhanced microporosity have been prepared *via* KOH activation. As the degree of activation increases, the micropore volume and BET surface area of the carbon gradually increased at the expense of the mesostructural order. Notably high micropore volume (1.0 mL g^{-1}) and BET area (2700 m^2 g^{-1}) could be achieved, while a significant amount of mesoporosity (0.4–0.8 mL g^{-1}) was retained. The activated mesoporous carbons possessing varied pore structures have been investigated for hydrogen adsorption at room temperature, in correlation with the carbon textural properties. The results show that hydrogen adsorption capacities are linearly proportional to the micropore volume and BET surface area. Notably, KOH activated mesoporous carbon exhibited a remarkably enhanced hydrogen adsorption capacity (up to 0.75 wt% at 100 atm) as compared to the value of 0.3 wt% of pristine mesoporous carbon. Nevertheless, the capacity remains far short of the US DOE target of 6.5 wt%. Simple extrapolation of the experimental results indicates that room-temperature hydrogen physisorption on carbon-based materials would be less than 2.5 wt%. The results suggest that room-temperature hydrogen physisorption on nanoporous carbon would be inappropriate to meet the current DOE target.

Acknowledgements

This work was supported in part by the Creative Research Initiative Program of the Korean Ministry of Science and Technology and by School of Molecular Science through the Brain Korea 21 project.

References

1 R. Ryoo, S. H. Joo and S. Jun, *J. Phys. Chem. B*, 1999, **103**, 7743.
2 S. Jun, S. H. Joo, R. Ryoo, M. Kruk, M. Jaroniec, Z. Liu, T. Ohsuna and O. Terasaki, *J. Am. Chem. Soc.*, 2000, **122**, 10712.
3 S. H. Joo, S. J. Choi, I. Oh, J. Kwak, Z. Liu, O. Terasaki and R. Ryoo, *Nature*, 2001, **412**, 169.
4 T.-W. Kim, F. Kleitz, B. Paul and R. Ryoo, *J. Am. Chem. Soc.*, 2005, **127**, 7601.
5 T.-W. Kim, I.-S. Park and R. Ryoo, *Angew. Chem., Int. Ed.*, 2003, **42**, 4375.
6 M. Hartmann, A. Vinu and G. Chandrasekar, *Chem. Mater.*, 2005, **17**, 829.
7 A. Vinu, C. Streb, V. Murugesan and M. Hartmann, *J. Phys. Chem. B*, 2003, **107**, 8297.
8 W. Xing, S. Z. Qiao, R. G. Ding, F. Li, G. Q. Lu, Z. F. Yan and H. M. Cheng, *Carbon*, 2006, **44**, 216.
9 C. Vix-Guterl, S. Saadallah, K. Jurewicz, E. Frackowiak, M. Reda, J. Parmentier, J. Patarin and F. Beguin, *Mater. Sci. Eng., B*, 2004, **108**, 148.
10 R. Gadiou, S.-E. Saadallah, T. Piquero, P. David, J. Parmentier and C. Vix-Guterl, *Microporous Mesoporous Mater.*, 2005, **79**, 121.
11 S. C. Laha and R. Ryoo, *Chem. Commun.*, 2003, 2138.
12 A. Sakthivel, S.-J. Huang, W.-H. Chen, Z.-H. Lan, K.-H. Chen, T.-W. Kim, R. Ryoo, A. S. T. Chiang and S.-B. Liu, *Chem. Mater.*, 2004, **16**, 3168.
13 M. J. Illán-Gómez, A. García-García, C. Salinas-Martínez de Lecea and A. Linares-Soano, *Energy Fuels*, 1996, **10**, 1108.
14 H. Teng and L.-Y. Hsu, *Ind. Eng. Chem. Res.*, 1999, **38**, 2947.
15 D. Lozano-Castelló, M. A. Lillo-Ródenas, D. Cazorla-Amorós and A. Linares-Soano, *Carbon*, 2001, **39**, 741.
16 E. Raymundo-Piñero, D. Cazorla-Amorós, A. Linares-Soano, S. Delpeux, E. Frackowiak, K. Szostak and F. Béguin, *Carbon*, 2002, **40**, 1597.
17 M. A. Lillo-Ródenas, J. Juan-Juan, D. Cazorla-Amorós and A. Linares-Soano, *Carbon*, 2004, **42**, 1371.
18 J. A. Marciá-Agulló, B. C. Moor, D. Cazorla-Amorós and A. Linares-Soano, *Carbon*, 2004, **42**, 1367.
19 L. Schlapbach and A. Züttel, *Nature*, 2001, **414**, 353.
20 A. Chambers, C. Park, T. K. Baker and N. M. Rodriguez, *J. Phys. Chem. B*, 1998, **102**, 4253.
21 A. C. Dillon, K. M. Jones, T. A. Bekkedahl, C. H. Klang, D. S. Bethune and M. J. Heben, *Nature*, 1997, **386**, 377.
22 Q. Wang and J. K. Johnson, *J. Chem. Phys.*, 1999, **110**, 577.
23 M. Rzepka, P. Lamp and M. A. de la Casa-Lillo, *J. Phys. Chem. B*, 1998, **102**, 10894.
24 M. Rzepka, E. Bauer, G. Reichenauer, T. Schliermann, B. Bernhardt, K. Bohmhammel, E. Henneberg, U. Knoll, H.-E. Maneck and W. Braue, *J. Phys. Chem. B*, 2005, **109**, 14979.
25 P. Chen, X. Wu, J. Lin and K. L. Tan, *Science*, 1999, **285**, 91.
26 R. T. Yang, *Carbon*, 2000, **38**, 623.
27 A. Lan and A. Mukasyan, *J. Phys. Chem. B*, 2005, **109**, 16011.
28 M. Dubinin, *Carbon*, 1983, **21**, 359.
29 G. Horvath and K. Kawazoe, *J. Chem. Eng. Jpn.*, 1983, **16**, 470.
30 E. P. Barrett, L. S. Joyner and P. P. Halenda, *J. Am. Chem. Soc.*, 1951, **73**, 373.
31 M. A. de la Casa-Lillo, F. Lamari-Darkrim, D. Cazorla-Amorós and A. Linares-Soano, *J. Phys. Chem. B*, 2002, **106**, 10930.
32 H. K. Chae, D. Y. Siberio-Perez, J. Kim, Y. Go, M. Eddaoudi, A. J. Matzger, M. ÒKeeffe and O. M. Yaghi, *Nature*, 2004, **427**, 523.
33 B. Panella, M. Hirscher and S. Roth, *Carbon*, 2005, **43**, 2209.
34 P. Kowalczyk, H. Tanaka, R. Holyst, K. Kaneko, T. Ohmori and J. Miyamoto, *J. Phys. Chem. B*, 2005, **109**, 17174.
35 Y. Li and R. T. Yang, *J. Am. Chem. Soc.*, 2006, **128**, 726.
36 E. Frackowiak and F. Béguin, *Carbon*, 2002, **40**, 1775.
37 C. Vix-Guterl, E. Frackowiak, K. Jurewicz, M. Friebe, J. Parmentier and F. Béguin, *Carbon*, 2005, **43**, 1293.
38 B. Fang, H. Zhou and I. Honma, *J. Phys. Chem. B*, 2006, **110**, 4875.